Low-temperature damping behavior of cast iron with aluminum addition

XINBAO LIU*, SUSUMU TAKAMORI, YOSHIAKI OSAWA, FUXING YIN
Eco-Circulation Processing Materials Group, National Institute for Materials Science, Tsukuba, Ibaraki 305-0047, Japan
E-mail: xbliu_76@hotmail.com

Recently, many investigations found that the damping capacity of cast iron is due to dislocation processes in the graphite inclusions. The experimental results of Adams and Fox [1, 2] indicated that at room temperature, the high-damping capacity for flake-graphite cast iron occurs principally within the graphite rather than the matrix or the matrix-graphite interface. Millet [3–5] further confirmed that this conjecture by comparing the internal friction spectra of cast iron and graphite, which were both characterized by a drastic increase in damping capacity from a relatively low level for $T < 200$ K to relatively high level for $T > 250$ K.

However, cast iron can exist in a great number of different forms depending on the chemical composition, the degree of nucleation of melt and casting conditions. If the carbon equivalent was suitable or if there were appreciable quantities of graphite stabilizing elements, then the carbon solidified mainly as the free graphite. It was known that aluminum was a graphite stabilizing elements, which favored the graphite formation. Correspondingly, the cast iron with aluminum addition had a high damping capacity at room temperature [6–8]. But the damping capacity at room temperature was connected with the evolution of the low-temperature internal friction spectrum. Therefore, it is necessary to study the low-temperature damping capacity of cast iron with aluminum addition.

In the present work, the damping behavior of cast iron with aluminum addition at low temperatures was investigated in detail. Meanwhile, the effect of aluminum on the damping capacity of cast iron was analyzed.

The compositions of the cast iron specimens used in the experiments were listed in Table I. High purity iron, carbon, silicon and aluminum (purity better than 99.9%) were used to prepare samples. The melting process was carried out in an induction-melting furnace and then the melts were cast into the sand mold. In order to remove the residual stress of cast iron, some samples were annealed at 873 K for 2 hr and continuously cooled to room temperature in a sealed quartz tube. Model 2980 DMA was used to measure the damping capacity of samples by the methods of dual cantilever with the mode of temperature and frequency sweeping under a fixed strain amplitude. Meanwhile, the Young's modulus of the materials was tested. The surface strain amplitude of the specimen was sustained at about 2.0×10^{-5} when heating the samples from 123 K to 373 K with a heating rate 5 K/min. Before the damping measurement, all the samples were cut into beam shapes, $1 \times 10 \times 60$ mm^3, and then were symmetrically bonded to the clamp. The damping capacity was evaluated by the tangent of phase lag, ϕ, between the stress and strain. It was expressed as:

$$Q^{-1} = \tan\phi \tag{1}$$

where Q^{-1} represents the internal friction.

Fig. 1 shows the temperature dependent variations of damping capacity for the unannealed and annealed cast irons with different compositions under the oscillation frequency of 10 Hz, respectively. It can be clearly seen that the damping capacities of the cast iron with aluminum addition were larger than those of the cast iron without aluminum, which was mainly caused by the different shapes of graphite in both cast irons [8]. In all samples, there were two damping peaks, P_1 and P_2, near the temperatures of 168 and 237 K, respectively, and the heights of both peaks were sensitive to the heat treatment. In the cast iron without aluminum, the height of P_1 peak decreased and P_2 peak increased after the annealed treatment of the sample, which can be seen in Fig. 1a. On the contrary, the height of the P_1 peak increased and P_2 peak decreased in the annealed cast iron with aluminum addition (Fig. 1b). Besides, after heat treatment, the room-temperature damping capacity of the cast iron without aluminum increased and the variations of damping capacity of the cast iron with aluminum addition were opposite.

Fig. 2 presents the simultaneous variations of the Young's modulus of samples when measuring the damping capacity. It is obvious that the Young's moduli of cast irons without aluminum were larger than those of cast irons with aluminum addition. In all samples, there existed a large change of the Young's modulus at the temperatures of P_2 peak of damping capacity. And while, a relatively small change of the Young's

TABLE I Chemical composition of the cast iron samples (wt%)

Sample	*C*	Si	Al	Fe
1	3.2	2.4	0	Bal.
2	3.2	2.4	6	Bal.

*Author to whom all correspondence should be addressed.

0022–2461

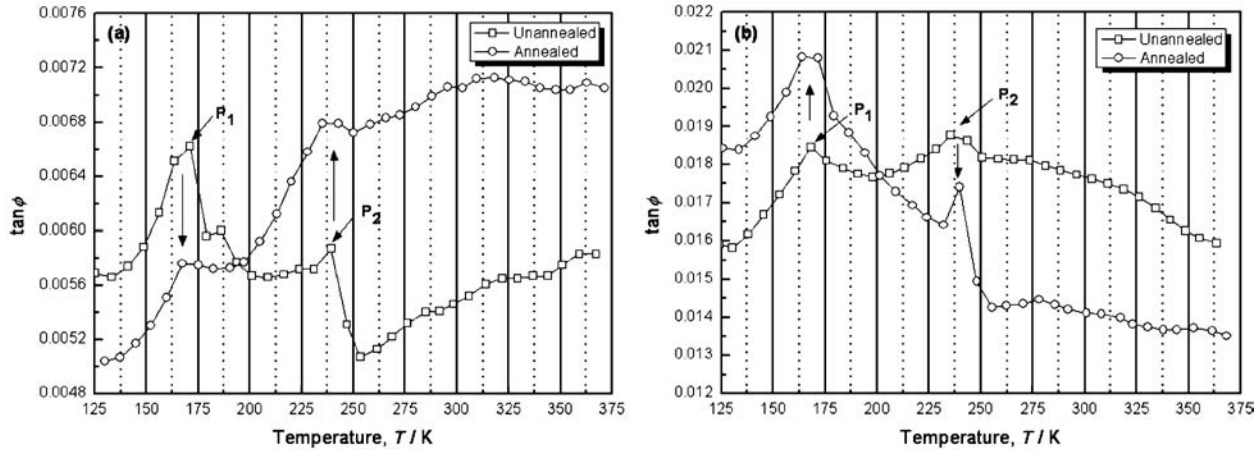

Figure 1 Influence of annealed treatment on temperature dependence of damping capacity in cast irons with (a) none aluminum and (b) 6% aluminum.

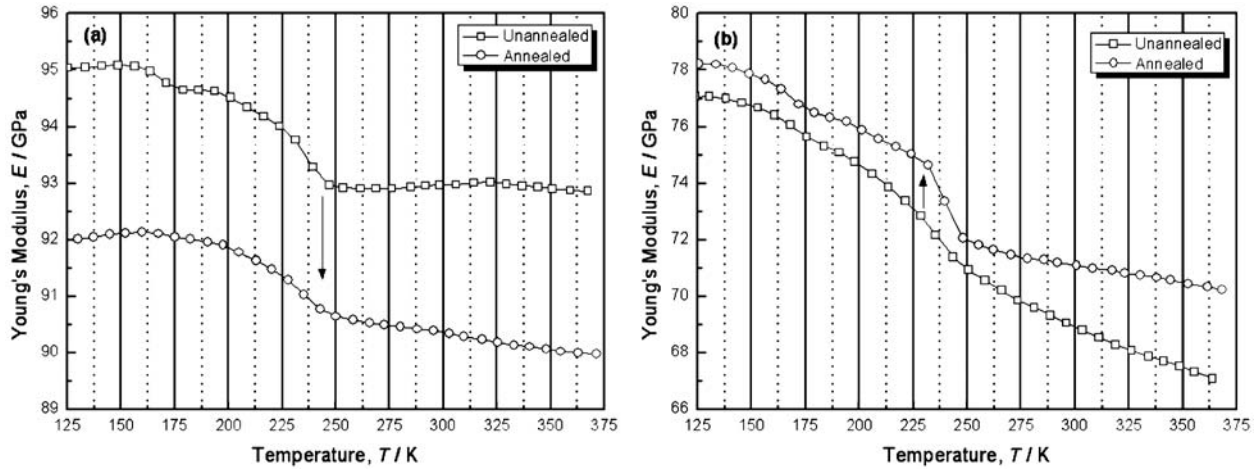

Figure 2 Influence of annealed treatment on temperature dependence of Young's modulus in cast irons with (a) none aluminum and (b) 6% aluminum.

modulus occurred in the unannealed cast iron without aluminum and the annealed cast iron with aluminum addition at the temperature of P_1 peak of damping capacity. Besides, compared with the unannealed sample, the Young's modulus decreased in the cast iron without aluminum (Fig. 2a). By contraries, the Young's modulus of the cast iron with aluminum addition increased by the annealed treatment (Fig. 2b).

All the above experimental results indicated that at low temperatures, there were two peaks, P_1 and P_2, for all samples in the temperature dependence of damping capacity. The annealed treatment had a large influence on the heights of both peaks. By the annealed treatment, the height of P_1 peak decreased and P_2 peak increased in the cast iron without aluminum and the opposite variations occurred in the cast irons with aluminum. In addition, with aluminum addition, the damping capacity of cast irons increased and the Young's modulus decreased.

Usually, the mechanical properties of a material were determined by its microstructure. The previous experiments indicated that the graphite play an important role in the damping capacity of cast iron [1, 2]. The coarser the graphite flake was, the higher the damping capacity. Recent investigations further confirmed that the damping capacity of cast iron is strongly under the control of dislocations of graphite [3–5]. Therefore, the formation of the two peaks, P_1 and P_2 at low temperatures was mainly attributed to the movements of dislocations within the graphite.

The common structure of graphite consisted of a hexagonal stacking of sheets of hexagonally linked carbon atoms in two different positions, *a* and *b*. The stacking sequence can be summarized as *abab*... [9]. As a function of temperature, the distance, *c*, between the basal planes, *a* and *b*, increased. At the lower temperature, this distance was small enough to pin the movements of the dislocations within the graphite [5]. Therefore, the formation of the damping P_1 peak at the lower temperature was due to the interaction between the vibration of dislocations within the graphite and the point defects. According to the vibrating string model [10], the damping capacity Q^{-1} and the Young's modulus $\Delta E/E$ can be given by

$$Q^{-1} = \frac{Bl^4\Lambda}{\pi^3 \mathrm{C}}\omega \tag{2}$$

$$\frac{\Delta E}{E} = \frac{l^2\Lambda}{\pi^2} \tag{3}$$

where B is the damping coefficient, l the mean dislocation loop length, Λ the dislocation density, C the line tension of dislocation and ω the angle frequency

of vibration. From the Equations (2) and (3), it can be seen that when the frequency was fixed, the damping capacity Q^{-1} and the Young's modulus $\Delta E/E$ were mainly determined by the density and length of the dislocations.

By the annealed treatment, the density and length of dislocations within the graphite greatly decreased in the cast iron without aluminum while the intrinsical point defects decreased. Combined with Equations (2) and (3), it can be deduced that the height of the damping capacity P_1 peak and the Young's modulus $\Delta E/E$ would decrease in the annealed cast iron without aluminum, which were consistent with the present experiment results (in Figs 1a and 2a). In the annealed cast iron with aluminum addition, there were much more dislocations within graphite because of the plastic deformation of the formation of a hard $Fe_3AlC_{0.5}$ phase during the annealed process [8, 11]. Consequently, the height of the damping P_1 peak and the Young's modulus $\Delta E/E$ increased, which can be seen in the Figs 1b and 2b, respectively.

With the increasing temperature, the distance, c, between the basal planes of graphite increased, which allowed the breakaway of dislocations from the pining points at a critical temperature. Millet [5] found that the critical temperature was within the range from 200 to 300 K, which includes the present temperature of P_2 peak. Therefore, it can be deduced that the damping P_2 peak was formed by the unpinned dislocation movements. From the G-L theory [12], the damping capacity Q^{-1} and the Young's modulus $\Delta E/E$ can be calculated by the following equations:

$$Q^{-1} = \frac{C_1}{\varepsilon_0} \exp\left(-\frac{C_2}{\varepsilon_0}\right) \tag{4}$$

$$\frac{\Delta E}{E} = \frac{12}{\pi^2} Q^{-1} \tag{5}$$

with $C_1 = (\Omega\Delta_0/\pi)(\Lambda L_N^3/L_d)C_2$, $C_2 = \pi^4 b\eta/L_d/96$. Ω is the orientation factor, b the Burger's vector, η the lattice mismatch coefficient, Δ_0 the distribution function of dislocations. Besides, L_N and L_d are the average loop lengths between unbreakable and breakable pins, respectively. By the Equation (4), it indicated that the damping capacity was mainly dependent on the exponent part. That is, the density of point defects, $1/L_d$, played an important role in the damping capacity. The smaller the density of point defects was, the larger the damping capacity

The annealed treatment made the intrinsical point defects decrease in all samples. On the other hand, the cementite in the annealed cast iron without aluminum was decomposed into graphite and ferrite. According to the Equation (4), the damping P_2 peak greatly increased and the Young's modulus decreased in the annealed cast iron without aluminum due to the both effects. In the cast iron with aluminum addition, the temperature of the eutectoid reaction increased, which made the cementite stable during the present treatment [8]. However, because of the formation of the hard $Fe_3AlC_{0.5}$ phase, the graphite content decreased and the dislocations increased [8]. Consequently, the damping P_2 peak decreased and the Young's modulus increased in the annealed cast iron with aluminum addition. In addition, because of increase of the graphite content, the damping capacity increased in the annealed cast iron without aluminum at room temperature. In the annealed cast iron with aluminum addition, the variation of damping capacity was opposite.

In this study, the low-temperature damping behavior of the cast iron with aluminum addition was investigated by the DMA method. Two damping peaks near the temperatures of 168 and 237 K were obtained in all samples, respectively. And while, there were relatively large variations of Young's modulus in the unannealed cast iron without aluminum and the annealed cast iron with aluminum addition at the temperatures of the both damping peaks. According to the vibrating string model and G-L theory, the low-temperature damping behavior of cast iron was discussed. It indicated that the lower temperature peak is attributed to the dislocation vibration within the graphite. The higher temperature peak is formed by the breakaway of dislocations. Besides, with aluminum addition, the variations of the damping capacity and Young's modulus in the annealed cast iron were diffierent due to various phase transformations.

Acknowledgements

This work was carried out under the financial supports of the Special Coordination Funds of Ministry, Culture, Sports, Science and Technology of Japanese Government.

References

1. R. D. ADAMS and M. A. O. FOX, *J. Iron Steel Inst.* **37** (1973) 4028.
2. M. A. O. FOX and R. D. ADAMS, *J. Mech. Eng. Sci.* **81** (1973).
3. P. MILLET, R. SCHALLER and W. BENOIT, *J de Phys.* **42** (1981) C5 929.
4. *Idem., ibid.* **44** (1983) C9 511.
5. *Idem., ibid.* **46** (1985) C10 405.
6. S. TAKAMORI, Y. OSAWA and K. HALADA, *Mater Trans. JIM* **43**(3) (2002) 311.
7. X. B. LIU, S. TAKAMORI and Y. OSAWA, to be published in *J. Mat. Sci. Lett.*
8. S. TAKAMORI, T. KIMURA and Y. OSAWA, *J. Japan Foundry Eng. Soc.* **74** (2002) 3.
9. S. AMELINCKX and P. DELAVIGNETTE, *J. Appl. Phys.* **31**(12) (1960) 2126.
10. A. GRANATO and K. LUCKE, *J. Appl. Phys.* **27**(6) (1956) 583.
11. A. RADHAKRISHNA, R. G. BALIGIDAD and D. S. SARMA, *Script. Mater.* **45** (2001) 1077.
12. D. ROGERS, *J. Appl. Phys.* **33**(3) (1962) 781.

Received 21 July
and accepted 18 August 2004